FINITE ELEMENT COMPUTATION OF UNSTEADY VISCOUS TRANSONIC FLOWS PAST AIRFOILS

S. Mittal
Department of Aerospace Engineering
Indian Institute of Technology
Kanpur, UP 208 016, INDIA

Abstract

In this article we present our results for computation of unsteady viscous transonic flows past stationary airfoils at various angles of attack. Stabilized finite element methods are employed to solve the compressible Navier-Stokes equations in their conservation law form. The non-linear equations resulting from the finite element discretizations are solved using the Generalized Minimal RESidual (GMRES) technique. Interesting flow patterns involving interactions between shock waves, boundary layers and shear layers are observed for all the cases. It is observed that the unsteadiness in the wake and the strength of the shocks involved increase with an increase in the angle of attack.

Keywords: Finite-elements, Transonic, Viscous, Airfoil, Vortex-shedding.

1 Introduction

Viscous transonic flows are associated with complex interactions between the boundary/shear layers and shock/expansion waves. In the transonic regime, the flows are quite sensitive to the free-stream Reynolds and Mach numbers; the boundary/shear layer behaviour mainly depends on the Reynolds number while the shock/expansion wave behaviour depends mainly on the Mach number [1, 2]. A number of numerical studies have been devoted to the analyses of steady inviscid transonic flows [3, 4, 5, 6, 7, 8]. Fewer studies have been conducted for unsteady, viscous flows [9, 10, 11, 12]. In this article, we present our results for the computation of unsteady viscous transonic flows past airfoils at various angles of attack.

We begin by reviewing the governing equations in Section 2. The equations are written in the conservation law form. The stabilized variational formulation of these equations in terms of the conservation variables is presented in Section 3. The SUPG (streamline-upwind/Petrov-Galerkin) stabilization technique is employed to stabilize our computations against spurious numerical oscillations due to advection dominated flows. The SUPG technique was first introduced by Hughes and Brooks [13] for the advection-diffusion equation and for incompressible flows. It was introduced in the context of inviscid compressible flows by Tezduyar and Hughes [7, 14] and Hughes and Tezduyar [3]. In addition to the SUPG stabilizations we supplement our formulation with a shock-capturing term to provide stability of the computations in the presence of discontinuities and large gradients in the flow. This idea, in the context of conservation variables, was demonstrated by Le Beau and Tezduyar [6]. In the current work we employ the same shock capturing operator as the one by Le Beau and Tezduyar [6] but with a modified coefficient to account for the unsteadiness in the flow. The effect of this modified term is demonstrated in [12] via a numerical example. In Section 4 we present our results for computation of flows past airfoils at various angles of attack.

2 The Governing Equations

Let $\Omega \subset \mathbb{R}^{n_{sd}}$ and $(0,T)$ be the spatial and temporal domains respectively, where n_{sd} is the number of space dimensions, and let Γ denote the boundary of Ω. The spatial and temporal coordinates are

denoted by $\mathbf{x}$ and t. The Navier-Stokes equations governing the fluid flow, in conservation form, are

$$\frac{\partial \rho}{\partial t} + \nabla \cdot (\rho \mathbf{u}) = 0 \qquad \text{on } \Omega \text{ for } (0,T), \tag{1}$$

$$\frac{\partial (\rho \mathbf{u})}{\partial t} + \nabla \cdot (\rho \mathbf{u}\mathbf{u}) + \nabla p - \nabla \cdot \mathbf{T} = \mathbf{0} \qquad \text{on } \Omega \text{ for } (0,T), \tag{2}$$

$$\frac{\partial (\rho e)}{\partial t} + \nabla \cdot (\rho e \mathbf{u}) + \nabla \cdot (p\mathbf{u}) - \nabla \cdot (\mathbf{T}\mathbf{u}) + \nabla \mathbf{q} = 0 \qquad \text{on } \Omega \text{ for } (0,T). \tag{3}$$

Here ρ, $\mathbf{u}$, p, $\mathbf{T}$, e, and $\mathbf{q}$ are the density, velocity, pressure, viscous stress tensor, the total energy per unit mass, and the heat flux vector, respectively. The viscous stress tensor is defined as

$$\mathbf{T} = \mu((\nabla \mathbf{u}) + (\nabla \mathbf{u})^T) + \lambda(\nabla \cdot \mathbf{u})\mathbf{I}. \tag{4}$$

where μ and λ are the viscosity coefficients. It is assumed that μ and λ are related by

$$\lambda = -\frac{2}{3}\mu. \tag{5}$$

Pressure is related to the other variables via the equation of state. For ideal gases, the equation of state assumes the special form

$$p = (\gamma - 1)\rho i, \tag{6}$$

where γ is the ratio of specific heats and i is the internal energy per unit mass that is related to the total energy per unit mass and velocity as

$$i = e - \frac{1}{2} \| \mathbf{u} \|^2 \tag{7}$$

The heat flux vector is defined as

$$\mathbf{q} = -\kappa \nabla \theta, \tag{8}$$

where κ is the heat conductivity and θ is the temperature. The temperature related to the internal energy by the following relation

$$\theta = \frac{Ri}{\gamma - 1}, \tag{9}$$

where R is the ideal gas constant. Prandtl number (P_r), assumed to be specified, relates the heat conductivity to the fluid viscosity according to the following relation

$$\kappa = \frac{\gamma R \mu}{(\gamma - 1)P_r}. \tag{10}$$

The compressible Navier-Stokes equations (1), (2), and (3) can be written in the conservation variables

$$\frac{\partial \mathbf{U}}{\partial t} + \frac{\partial \mathbf{F}_i}{\partial x_i} - \frac{\partial \mathbf{E}_i}{\partial x_i} = \mathbf{0} \qquad \text{on } \Omega \text{ for } (0,T), \tag{11}$$

where $\mathbf{U} = (\rho, \rho u_1, \rho u_2, \rho e)$, is the vector of conservation variables, and $\mathbf{F}_i$ and $\mathbf{E}_i$ are, respectively, the Euler and viscous flux vectors defined as

$$\mathbf{F}_i = \begin{pmatrix} u_i \rho \\ u_i \rho u_1 + \delta_{i1} p \\ u_i \rho u_2 + \delta_{i2} p \\ u_i (\rho e + p) \end{pmatrix} \tag{12}$$

$$\mathbf{E}_i = \begin{pmatrix} 0 \\ \tau_{i1} \\ \tau_{i2} \\ q_i + \tau_{ik} u_k \end{pmatrix} \tag{13}$$

Here u_i, q_i, and τ_{ik} are the components of the velocity, heat flux, and viscous stress tensor, respectively. In the quasi-linear form, equation (11) is written as

$$\frac{\partial \mathbf{U}}{\partial t} + \mathbf{A}_i \frac{\partial \mathbf{U}}{\partial x_i} - \frac{\partial}{\partial x_i}\left(\mathbf{K}_{ij}\frac{\partial \mathbf{U}}{\partial x_j}\right) \quad 0 \qquad \text{on } \Omega\, f\langle \quad 0, T \rangle \tag{14}$$

where

$$\mathbf{A}_i = \frac{\partial \mathbf{F}_i}{\partial \mathbf{U}},$$

is the Euler Jacobian Matrix, and $\mathbf{K}_{ij}$ is the diffusivity matrix satisfying

$$\mathbf{K}_{ij}\frac{\partial \mathbf{U}}{\partial x_i} = \mathbf{E}_i. \tag{16}$$

Corresponding to equation (14), the following boundary and initial conditions are chosen

$$\mathbf{U} = \mathbf{g} \qquad \text{on } \Gamma_g \; for \; (0,T), \tag{17}$$

$$\mathbf{n}\cdot\mathbf{E} = \mathbf{h} \qquad \text{on } \Gamma_h \; for \; (0,T), \tag{18}$$

$$\mathbf{U}(\mathbf{x},0) = \mathbf{U_0} \qquad \text{on } \Omega_0. \tag{19}$$

Subscript g refers to Dirichlet boundary conditions while the subscript h refers to the Neumann boundary conditions. The specification of these conditions for the flow past an airfoil is described in Section 4.

3 Finite Element 'ormulation

Consider a finite element discretization of Ω into subdomains Ω^e, $e = 1, 2, ..., n_{el}$, where n_{el} is the number of elements. Based on this discretization, we define the finite element trial function space $\mathcal{S}^h$ and weighting function space $\mathcal{V}^h$. These function spaces are selected, by taking the Dirichlet boundary conditions into account, as subsets of $[\mathbf{H}^{1h}(\Omega)]^{n_{dof}}$, where $\mathbf{H}^{1h}(\Omega)$ is the finite-dimensional function space over Ω and n_{dof} is the number of degrees of freedom.

$$\in [\mathbf{H}$$

$$\mathcal{V}^h = \{\mathbf{W}^h | \mathbf{W}^h \in [\mathbf{H}^{1h}(\Omega)]^{n_{dof}}, \mathbf{W}^h|_{\Omega^e} \in [P^1(\Omega^e)] \qquad \mathbf{W}$$

wher $(\Omega^e)]$ represents the first order polynomial in Ω^e. stabiliz
elem ormulation of Eq. (14) is written as follows: find U uch that $\forall \mathbf{W}$

$$\mathbf{W} \quad \frac{\partial \mathbf{U}}{\partial t} + \mathbf{A} \qquad \frac{\partial \mathbf{W}}{\partial x_i} \qquad \mathbf{K}$$

$$\sum_{e=1}^{n_{el}} \int_{\Omega^e} \tau(\mathbf{A}_k^h \left(\frac{\partial \mathbf{W}^h}{\partial x_k}\right) \left[\frac{\partial \mathbf{U}^h}{\partial t} + \mathbf{A}_i^h \frac{\partial \mathbf{U}^h}{\partial x_i} \quad \frac{\partial}{\partial x_i}\left(\mathbf{K} \quad \frac{\partial \mathbf{U}^h}{\partial x_j}\right)\right] d\Omega$$

$$\sum_{e=1}^{\cdots el} {}_{J\Omega^e} \left\backslash \frac{\partial \mathbf{W}}{\partial x_i} \right/ \left\backslash \frac{\partial \mathbf{U}}{\partial x_i} \right/ \qquad {}_{J\Gamma_h} \mathbf{W} \quad \mathbf{h}$$

In the above formulation, the first two terms and the right-hand-side constitute the Galerkin formulation of the problem. The first series of element-level integrals are the SUPG stabilization terms added to the variational formulation to stabilize the computations against node-to-node oscillations in the advection-dominated range. The second series of element level integrals in the formulation are the shock capturing terms that stabilize the computations in the presence of sharp gradients. The interested reader is refered to [6, 15, 12] for more details on the formulation.

4 Numerical Simulations

All the computations reported in this article are carried out on *Digital* work-stations at *IIT Kanpur*. The method has already been tested on various benchmark problems [11, 12]. The non-linear equation systems resulting from the finite-element discretization of the flow equations are solved using the Generalized Minimal RESidual (*GMRES*) technique [16] in conjunction with diagonal and block-diagonal preconditioners. The Prandtl Number for all the cases in 0.72.

A NACA 0012 airfoil is placed in a *Mach* 0.85 flow. The Reynolds number, based on the chord of the airfoil, the free-stream velocity and kinematic viscosity is 10,000. Two meshes are employed to carry out the computations. The first mesh consists of 18,772 quadrilateral elements and 19,014 nodes. The upstream and down stream boundaries are located at 4.25 and 7.75 chord-lengths, respectively, while the upper and lower boundaries are 4.25 chord lengths away, each, with respect to the mid-chord point of the airfoil. This mesh is used to compute flows for the cases when the angles of attack are 0^o, 2^o and 5^o. As the angle of attack increases, it is felt that the size of the present domain, in the cross-flow direction, is inadequate. Therefore, a second mesh was employed which is identical to the first one close to the airfoil. In this case, the upper and lower boundaries are 12 chord lengths away, each, from the mid-chord point of the airfoil. This mesh consists of 22,132 quadrilateral elements and 22,414 nodes. Flows at angles of attack 8^o and 10^o are computed using this mesh.

The boundary conditions are prescribed as shown in the Figure 1. The computations are initiated with free-stream conditions in the entire domain. A time step of 0.01 is used to ensure time-accuracy of the results. On a *Digital* 250 – 4/266 workstation, each time-step takes approximately 1 minute of *CPU* time.

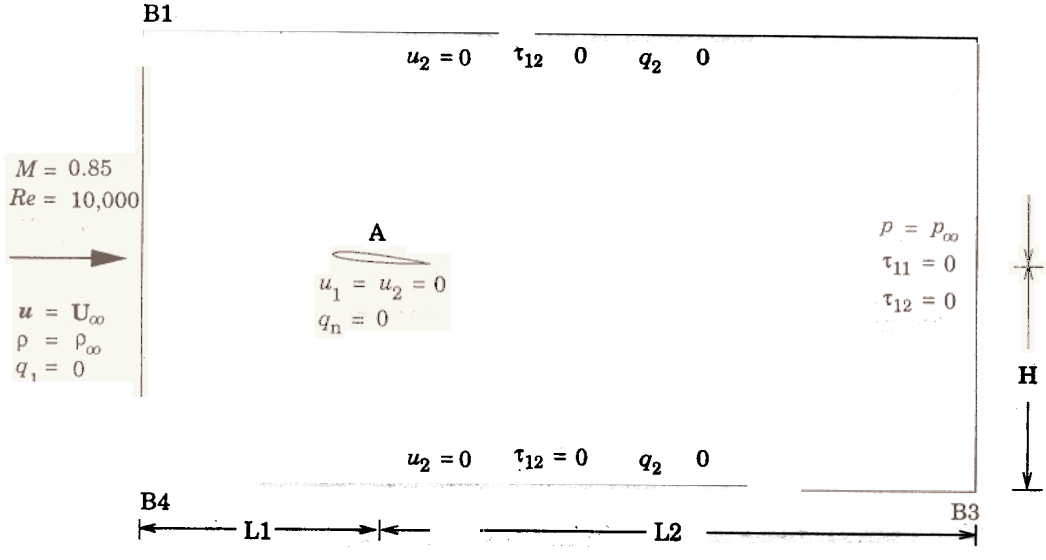

Figure 1: Flow past an airfoil in a channel: problem description

Figures 2–6 show the computed flow fields (density, temperature and pressure) at the peak value of lift coefficient for the temporally periodic solution. Figure 7 shows the time histories of the lift and drag coefficients for the flow past an airfoil at various angles of attack. It should be noted that the chord-length of the airfoil (and not its thickness) has been used to obtain the nondimensional quantities.

Figure 2 shows the flow field for the $\alpha = 0^o$ case. The interaction between the shock and expansion waves, and the boundary and shear layers can be clearly observed. Downstream of the front stagnation point, the flow accelerates and becomes supersonic. At, approximately, the mid-chord point, the

boundary layer thickens sufficiently enough to cause the flow to constrict resulting in the formation of a weak oblique shock. The interaction between the boundary layer and the shock wave results in the separation of flow and one can observe the formation of a shear layer downstream of the shock. Another shock is formed further downstream that combines with the shock and expansion waves formed upstream resulting in a lambda shock. In the wake region two kinds of flow instability mechanisms are active. One is the Kelvin-Helmoltz instability, associated with the shear layers, and the other is the interaction between the shear layer and the shock wave that is also responsible for transonic buffeting. Our flow patterns compare quite well with the computational results reported in [9] and with the experimental results in [17]. It must be pointed out that the laboratory experiments [17] were carried out at a much larger Reynolds number. Figure 7 shows the time histories of the lift and drag coefficients for this computation. The Strouhal number corresponding to the lift coefficient variation is 1.58. It can be observed that the drag coefficient oscillates at twice the frequency of the lift coefficient. This is consistent with the observation that the vortices are shed from both, the upper and the lower surfaces of the airfoil.

Solutions for flows at angles of attack 2^o, 5^o and 8^o 10^o are shown in Figures 3–7. From these figures it can be observed that as the angle of attack increases, the unsteadiness of the flow in the wake also increases, the lambda shock becomes stronger and, as expected, encompasses a larger region in the flow. At larger angles of attack, the flow at the upper surface of the airfoil separates quite close to the leading edge of the airfoil while the flow remains attatched on the lower surface. The vortex shedding takes place aft of the trailing edge of the airfoil as a result of the interaction between the shock wave and the shear layer.

5 Conclusions

Results have been presented for the computation of unsteady, laminar, viscous transonic flows past stationary airfoils at various angles of attack. The computations involve long-time integration of the Navier-Stokes equations and demonstrate that the boundary conditions utilized are quite robust. The results show interesting flow patterns and a complex interaction between the boundary/shear layers and shock/expansion waves. The unsteadiness in the flow increases with an increase in the angle of attack.

6 Acknowledgment

Partial support for this work has come from the Aeronautical Development Agency, India under the project number ADA-AE-95204. The author would also like to thank Prof. N.L. Arora, Department of Aerospace Engineering, IIT Kanpur, for providing access to his computational resources.

References

[1] H. Schlichting. *Boundary-Layer Theory.* McGraw-Hill, New York, 7th edition, 1979.

[2] A.M. Kuethe and C.Y. Chow. *Foundations of Aerodynamics. Bases of Aerodynamic Design.* John Wiley and Sons, New York, 1932.

[3] T.J.R Hughes and T.E. Tezduyar. Finite element methods for first-order hyperbolic systems with particular emphasis on the compressible Euler equations. *Computer Methods in Applied Mechanics and Engineering*, 45:217–284, 1984.

[4] M.O. Bristeau, O. Pironneau, R. Glowinski, J. Periaux, P. Perrier, and G. Poirier. On the numerical solution of nonlinear problems in fluid dynamics by least squares and finite element methods (II). Application to transonic flow simulations. *Computer Methods in Applied Mechanics and Engineering*, 51:363–394, 1985.

5] R. Lohner, K. Morgan, and O.C. Zienkiewicz. An adaptive finite element procedure for compressible high speed flows. *Computer Methods in Applied Mechanics and Engineering*, 51:441–465, 1985.

[6] G.J. Le Beau and T.E. Tezduyar. Finite element computation of compressible flows with the SUPG formulation. In M.N. Dhaubhadel, M.S. Engelman, and J.N. Reddy, editors, *Advances in Finite Element Analysis in Fluid Dynamics*, FED-Vol.123, pages 21–27, New York, 1991. ASME.

T.E. Tezduyar and T.J.R. Hughes. Finite element formulations for convection dominated flows with particular emphasis on the compressible Euler equations. In *Proceedings of AIAA 21st Aerospace Sciences Meeting*, AIAA Paper 83-0125, Reno, Nevada, 1983.

[8] J. Peraire, J. Peiro, and K. Morgan. Finite element multigrid solution of Euler flows past installed aero-engines. *Computational Mechanics*, 11:433–451, 1993.

[9] M.O. Bristeau, R. Glowinski, J. Periaux, and H. Viviand. GAMM-workshop: Numerical simulation of compressible Navier-Stokes flows; Presentation of problems and discussion of results. In Michel Deville, editor, *Notes on Numerical Fluid Mechanics: Proceedings of the Seventh GAMM-Conference on Numerical Methods in Fluid Mechanics*, volume 20 of *Notes on Numerical Fluid Mechanics*, pages 442–450. Vieweg, Wiesbaden, 1988.

10] S. Boivin and M. Fortin. A new artificial viscosity method for compressible viscous flow simulations by FEM. *International Journal of Computational Fluid Dynamics*, 1:25–41, 1993.

1] S.K. Aliabadi and T.E. Tezduyar. Space-time finite element computation of compressible flows involving moving boundaries and interfaces. *Computer Methods in Applied Mechanics and Engineering*, 107(1–2):209–224, 1993.

[12] S. Mittal. Finite element computation of unsteady viscous compressible flows. submitted to *Computer Methods in Applied Mechanics and Engineering*, 1996.

[13] T.J.R. Hughes and A.N. Brooks. A multi-dimensional upwind scheme with no crosswind diffusion. In T.J.R. Hughes, editor, *Finite Element Methods for Convection Dominated Flows*, AMD-Vol.34, pages 19–35. ASME, New York, 1979.

T.E. Tezduyar and T.J.R. Hughes. Development of time-accurate finite element techniques for first-order hyperbolic systems with particular emphasis on the compressible Euler equations. report prepared under NASA-Ames University Consortium Interchange, No. NCA2-OR745-104, 1982.

15] S.K. Aliabadi, S.E. Ray, and T.E. Tezduyar. SUPG finite element computation of compressible flows with the entropy and conservation variables formulations. *Computational Mechanics* 11:300–312, 1993.

16] Y. Saad and M. Schultz. GMRES: A generalized minimal residual algorithm for solving nonsymmetric linear systems. *SIAM Journal of Scientific and Statistical Computing*, 7:856–869, 1986.

[17] A. H. Shapiro. *The Dynamics and Thermodynamics of Compressible Fluid Flows*. The Ronald Press Company, New York, 1958.

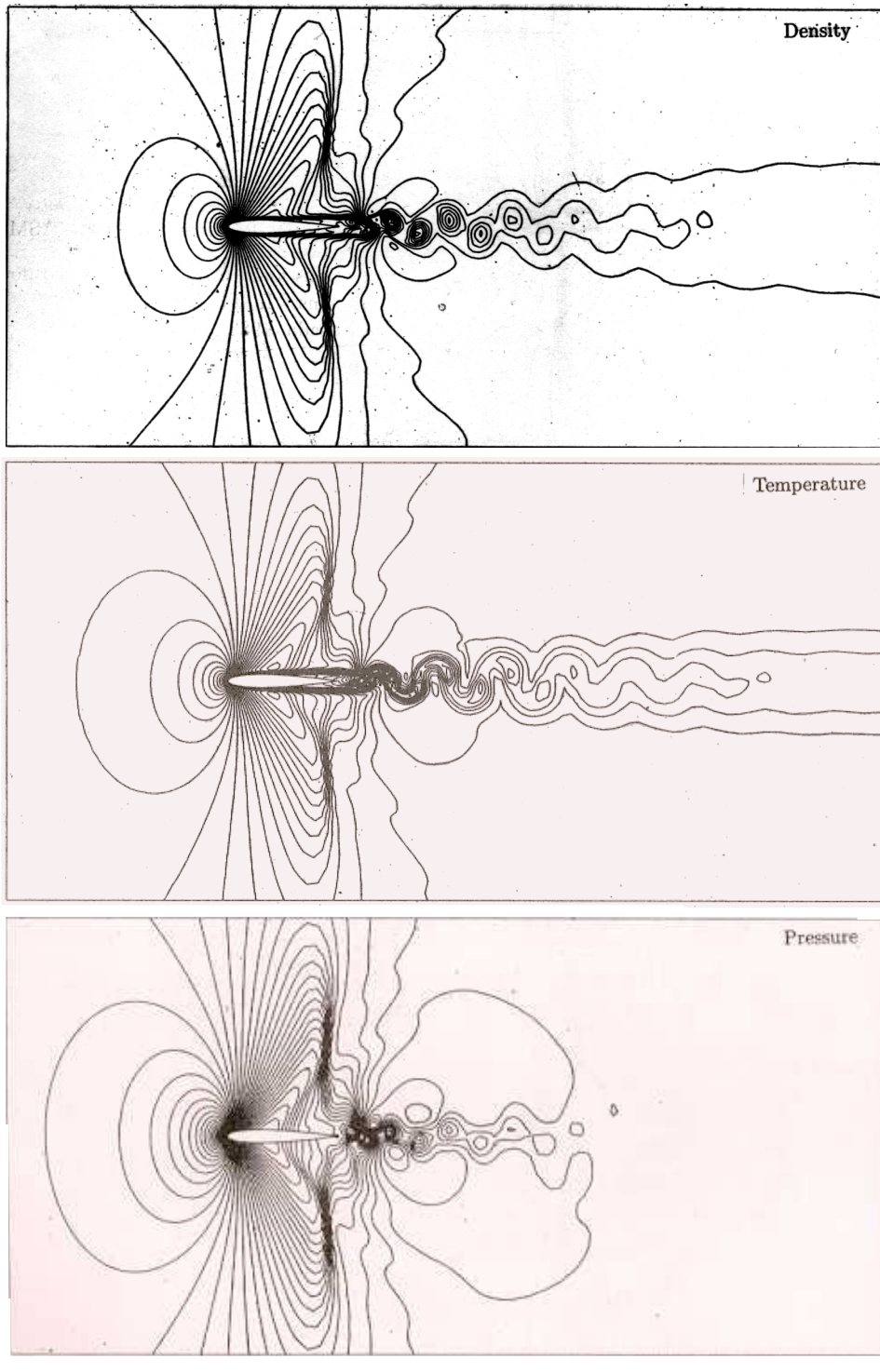

Figure 2: Mach=0.85, Re=10,000, $\alpha = 0°$ flow past a NACA0012 airfoil: density, temperature and pressure fields for the solution corresponding to the peak value of the lift coefficient.

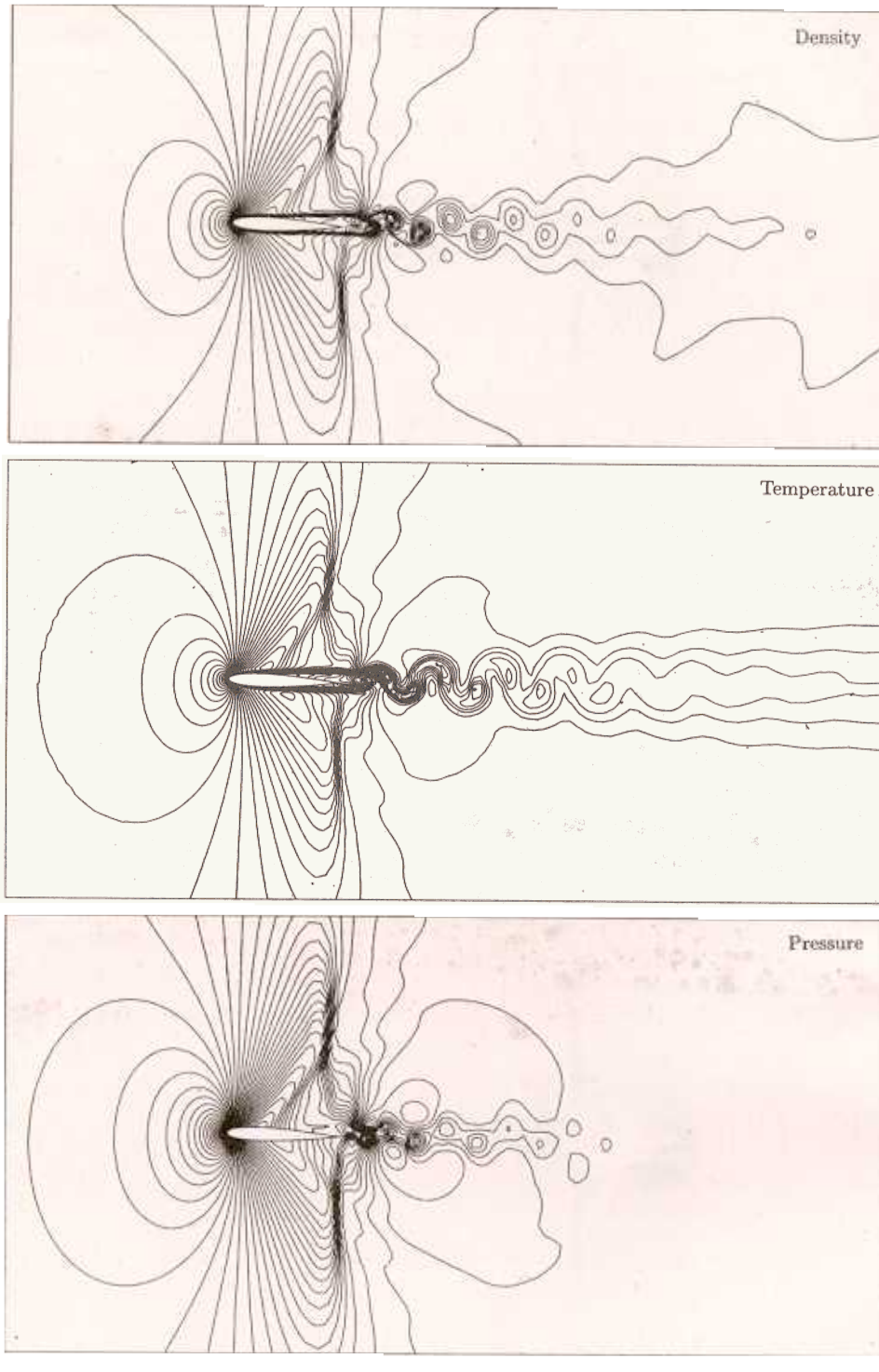

Figure 3: Mach=0.85, Re=10,000, $\alpha = 2^o$ flow past a NACA0012 airfoil: density, temperature and pressure fields for the solution corresponding to the peak value of the lift coefficient.

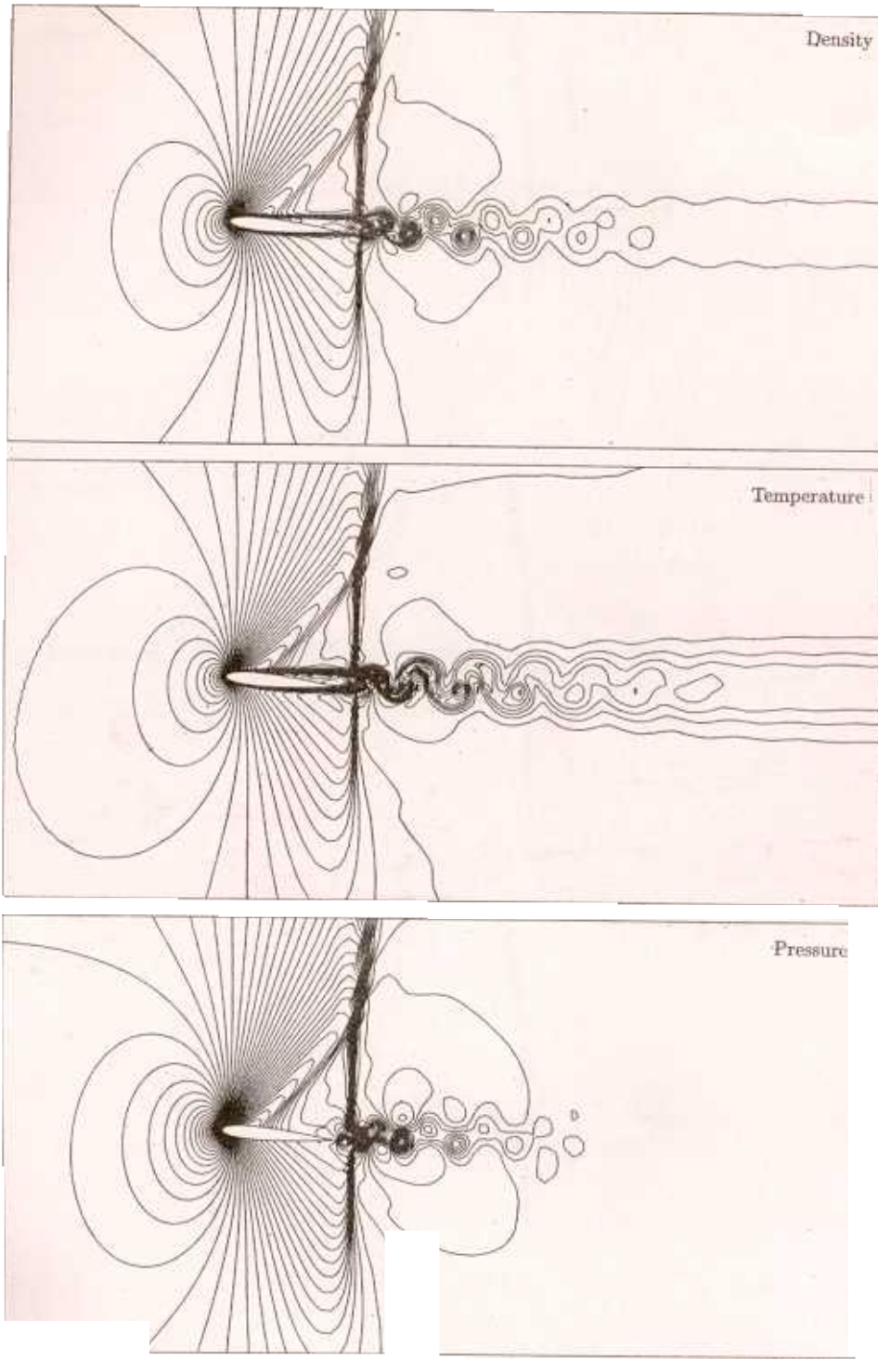

Figure 4: Mach=0.85, Re=10,000, $\alpha = 5^{o}$ flow past a NACA0012 airfoil: density, temperature and pressure fields for the solution corresponding to the peak value of the lift coefficient.

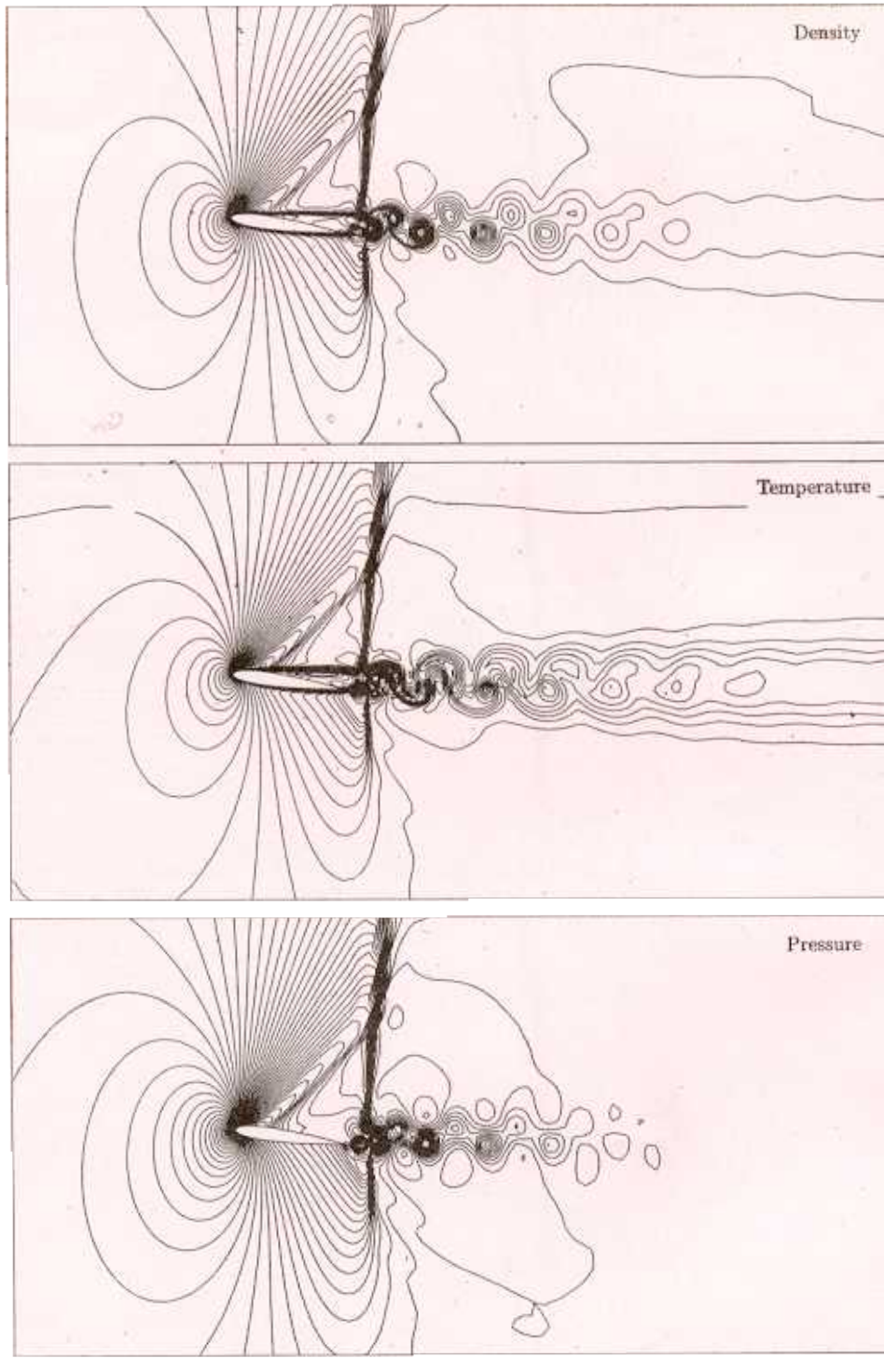

Figure 5: Mach=0.85, Re=10,000, $\alpha = 8°$ flow past a NACA0012 airfoil: density, temperature and pressure fields for the solution corresponding to the peak value of the lift coefficient.

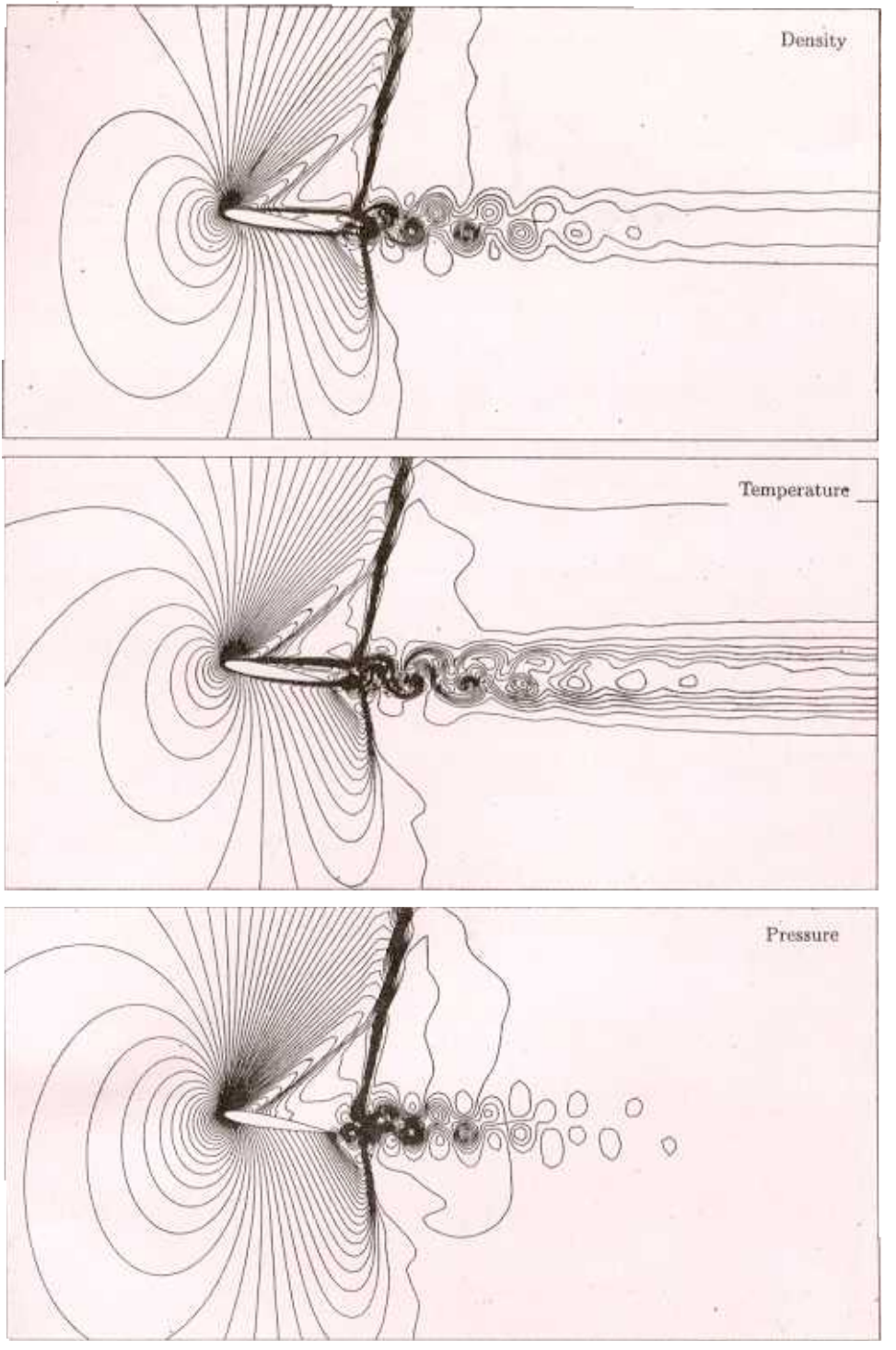

Figure 6: Mach=0.85, Re=10,000, $\alpha = 10^o$ flow past a NACA0012 airfoil: density, temperature and pressure fields for the solution corresponding to the peak value of the lift coefficient.

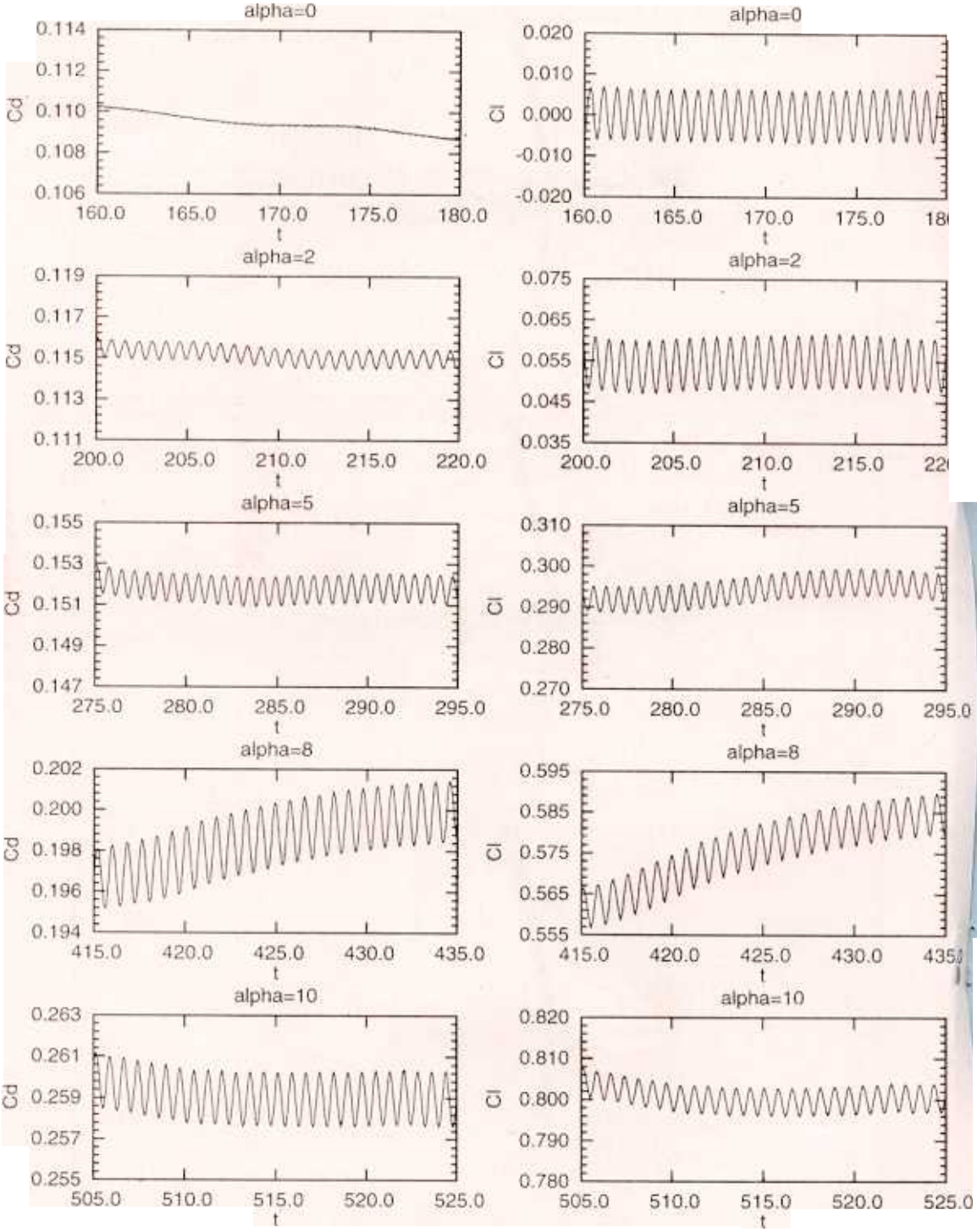

Figure 7: Mach=0.85, Re=10.000 flow past a NACA0012 airfoil: time histories of the drag and lift coefficients at various angles of attack.